Analytical Description of Anti-scattering and Scattering Bar Assist Features

John S. Petersen

Petersen Advanced Lithography Inc.

8834 North Capital of Texas Highway, Suite 301, Austin, TX 78759
www.advlitho.com; jpetersen@advlitho.com

Assist features are an essential component for developing an integrated imaging system that can produce near resolution limit sized semiconductor features. Of the features in use today, binary and phase-shifted scattering and anti-scattering bars are proving critical to the success of making current and next generation devices in production. These features modify the diffraction pattern of isolated lines to give them some dense line imaging attributes thus making it easier to overlap and enhance the process window for these features. They have also been shown to reduce the mask error enhancement factor and the effect of aberrations. This paper provides an analytic description of these assist features and uses this description to explain how and why these features work. Working in frequency space, it also demonstrates how to use these assist features with illuminator and phase-shift mask image enhancement techniques to build a robust semiconductor imaging process.

Key word: Assist Features, scattering bars, optical proximity correction, OPC, phase shift mask, binary mask, Fourier analysis

Introduction:

The use of sub-resolution assist features in microlithography is known to provide optical proximity compensation and improve depth of focus, reduce the mask error enhancement factor (MEEF), minimize the effect of aberrations and boost isolated line performance with off-axis illumination. E. A. Saleh published the first paper [1], where the use of compensation was first discussed to control corners using serifs and narrowing at line intersections. Next assist features in proximity or adjacent to the primary feature were used to form weak phase-shift masks.[2, 3, 4, 5, 6, 7, 8, 9, 10, 11] Later, binary scattering bars, which are opaque or semitransparent features that are offset from primary features in the bright field, and anti-scattering bars, their dark field analogues, were introduced by Chen, et al as an optical proximity compensation technique and to improve depth of focus. .[12, 13, 14, 15] They have also been used to provide optical proximity compensation with strong phase shifting.[16] Later, it was shown that they could reduce MEEF [17, 18, 19, 20, 11] and aberrations.[11, 15] Finally, they have been shown to boost the performance of isolated line features using off-axis illumination.[9, 10, 21]

This paper provides a simple, one-dimensional analytic description of binary and phase-shifted embodiments of assist feature technology, but recognizes expansion to two-dimensional is a simple expansion of this theme. The analysis is based on examples from Wilson's book.[22] This result is then used to show how a sub-resolution assist features modifies the shape of an isolated feature and the impact of those changes. Then aspects of the modifications are examined within the context of building an integrated imaging system.
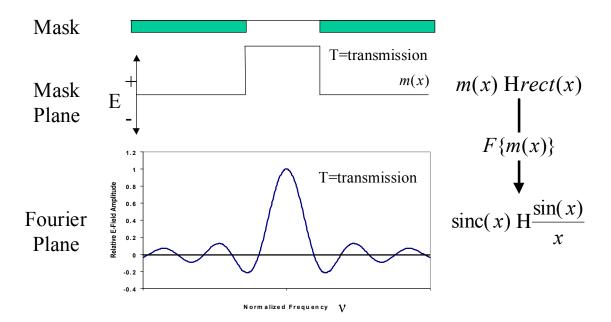
Figure 1 Cross section of mask with an isolated space. The electric field at the mask plane forms a rect(x). At the Fourier plane, the diffraction pattern is described by the Fourier transform of the rect(x) which is F{m(x)}= sinc(x) function.

Analytical Description

Figure 1 shows a cross sectional view of an isolated space on a photomask, of width, w_P, centered about x=0. In this figure, the shape of the electric field that is formed when coherent energy is passed through the slot is shown at the mask and at the pupil plane. At the mask plane the electric field can be described as a rect function of the horizontal distance, x. Rect(x) is zero everywhere except in the region between the edges of the space where it is not zero, and there, is proportional to the complex transparency of the mask. In the pupil plane of the lens, the isolated feature has a diffraction pattern that is described by the Fourier transform M(ν) or F{m(x)} of rect(x) which is sin(x)/x and is called sinc(x). The Fourier analysis transforms x-dimensional space to frequency space, ν. The Fourier transform is shown in Equation 1.

Equation 1
$$M(\nu) = F\{m(x)\} = \int_{-\infty}^{+\infty} m(x)e^{-i2\pi\nu x}dx$$

In this work, frequency is normalized to the range $-nNA/\lambda$ to $+nNA/\lambda$, where **n** is a scaling factor for the calculation that typically ranges from one to ten, NA is the numerical aperture of the pupil and λ is the actinic wavelength incident on the mask. Unless otherwise stated, the solutions in this work are based on coherent imaging. However, to see what might affect the image formation at the wafer, it is useful to set n=1+σ, where σ is the partial coherence of the imaging system. In this way, only the
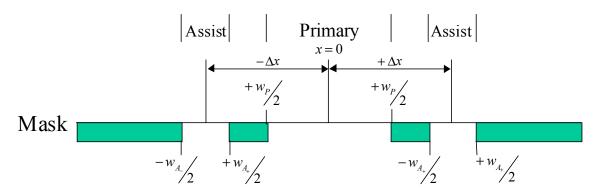
Figure 2 Cross-section of mask with a primary isolated space of width w_P, surrounded by sub-resolution assist features of width w_A with pitch of Δx.

range that can be accepted by NA is observed. The sinc function is everywhere in phase and can interfere to form the final image using any or all of the available interference angles contained within the sinc function envelope.

Figure 2 shows the isolated space with assist features added symmetrically about x=0. In this figure the width of the left and right assist features, w_L and w_R, respectively, are equal in size and transmittance. Like the primary, the assists can be described by their own sinc functions. They however are placed equidistant from the primary feature's center by Δx.

To derive the analytic solution for the assisted feature use superposition to solve $M(v)_{Total}$ by setting it equal to the sum of the individual transforms of $M(v)_{Primary}$, $M(v)_{Left}$ and $M(v)_{Right}$; where the assists are phase shifted relative to each other proportional to Δx, as defined by the Shift Theorem of Fourier Analysis. Mathematically, this sum is Equation 2.

Equation 2
$$M(v) = F\{m(x)\} = F\{P(x)\} + F\{A_{Left}(x + \Delta x)\} + F\{A_{Right}(x - \Delta x)\}$$
where v is frequency.

For the primary, centered at x=0, with width w_P and complex transmittance T_P, Equation 3:

Equation 3
$$F\{P(x)\} = \int_{-w_P/2}^{+w_P/2} P(x)e^{-i2\pi vx}dx = T_P \frac{\sin(\pi v w_P)}{\pi v}$$

$$\text{multiply } \frac{w_P}{w_P} \text{ to get sinc}(\pi x) \text{ to yield}:$$

$$F\{P(x)\} = T_P w_P \, \text{sinc}(\pi v w_P)$$

Now apply the Shift Theorem to the assist features, centered at x= $-\Delta x$ and $+\Delta x$, Equation 4a and 4b:

Equation 4a
$$F\{A_{Left}(x + \Delta x)\} =$$
$$T_{A_L} w_{A_L} e^{-i2\pi v \Delta x} \, \text{sinc}(\pi v w_{A_L})$$

Equation 4b

$$F\{A_{Right}(x-\Delta x)\} =$$

$$T_{A_R} w_{A_R} e^{+i2\pi v \Delta x} \operatorname{sinc}(\pi v w_{A_R})$$

Then using superposition, add all three spaces for a binary mask. If the assist features are asymmetric in w_A, T_A, or Δx, the solution is complex, Equation 5:

Equation 5

$$F\{m(x)\} = F\{P(x)\} + F\{A_{Right}(x-\Delta x)\} + F\{A_{Left}(x+\Delta x)\}$$

if assists features are different

$$= T_P w_P \operatorname{sinc}(\pi v w_P) + T_{A_L} w_{A_L} e^{-i2\pi v \Delta x} \operatorname{sinc}(\pi v w_{A_L})$$

$$+ T_{A_R} w_{A_R} e^{+i2\pi v \Delta x} \operatorname{sinc}(\pi v w_{A_R})$$

If the assist features are not asymmetric the solution is shown in Equation 6:

Equation 6

$$F\{m(x)\} =$$

$$= T_P w_P \operatorname{sinc}(\pi v w_P) + T_A w_A \operatorname{sinc}(\pi v w_A)(e^{+i2\pi v \Delta x} + e^{-i2\pi v \Delta x})$$

Using Euler's equation, Equation 6 is simplified to Equation 7:

Equation 7

$$= T_P w_P \operatorname{sinc}(\pi v w_P) + 2 T_A w_A \cos(2\pi v \Delta x) \operatorname{sinc}(\pi v w_A)$$

Phase-shifting can be examined simply by subtracting either the primary, Equation 8, or of the combined assist feature term, Equation 9.

Equation 8

$$F\{m(x)\} = -T_P w_P \operatorname{sinc}(\pi v w_P) + 2 T_A w_A \cos(2\pi v \Delta x) \operatorname{sinc}(\pi v w_A)$$

or

Equation 9

$$= T_P w_P \operatorname{sinc}(\pi v w_P) - 2 T_A w_A \cos(2\pi v \Delta x) \operatorname{sinc}(\pi v w_A)$$

Figure 3 shows a graphical representation of the binary solution for equation 7, Figure 5 shows a phase-shift solution for equation 9.

These are dark field solutions. To convert them to bright field subtract the dark field solution from a delta function, Equation 10.

Equation 10

$$F\{m(x)\}_{Bright-field} = \delta(v) - F\{m(x)\}_{Dark-field}$$

The examination of the analytic solutions will be restricted to the dark field cases in Equations 7 and 9.

Binary Examples

For binary masks, the dark field solution is shown by its components in Figure 3. This is a plot of relative electric field amplitude and the square of the amplitude versus
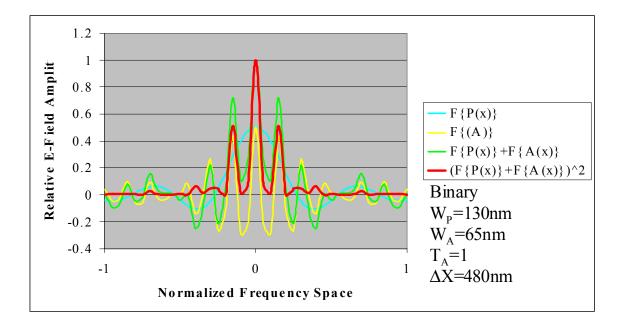
Figure 3 Plot of relative electric field amplitude and the square of the amplitude versus relative frequency, for n=10 for 130nm isolated space with 65nm assist features and complex transmittance of one. The amplitude is relative to the maximum amplitude of $F\{m(x)\}^2$. The curves show relative E-field amplitude contributions from the sinc function $F\{P(x)\}$, which is the transform of the primary feature, and from the sinc-shaped cosine function $F\{A(x)\}$ which is the transform of the assist features. Also shown are the sum of all the transforms, $F\{P(x)\} + F\{A(x)\}$, and the square of that sum, $F\{m(x)\}^2 = (F\{P(x) + F\{A(x)\})^2$.

relative frequency, for n=10 for a 130nm isolated space with 65nm assists and complex transmittance of one. The amplitude is relative to the square of the maximum amplitude of $F\{m(x)\}^2$. Figure 3 has four curves, the primary sinc, the cosine of the combined assist features that are shaped by the assist feature sinc, the sum of all the Fourier transforms and the square of that sum. Note that all sinc functions have a maximum at zero frequency and that the sum of all the transforms is a function that has side-lobes symmetrically placed around a strong central-lobe centered at zero frequency. While this function looks somewhat like the diffraction pattern of discrete orders formed by an infinite series of lines and spaces it is not discrete, it is still a sinc, albeit modified. This means that even if the central and side-lobes of the modified sinc function matches the frequency and amplitude of a dense line's diffraction pattern, it still contains the information of an isolated feature and will print as such.

Figure 4 shows how the sinc function is modified by the different parameters in Equation 7. The figure shows the relationship of w_P, w_A, T_A and Δx to the maximum amplitudes of the central and side-lobes, CL_Max and SL_Max, respectively, their ratio CL/SL; the minimum amplitude between the central-lobe and side-lobe maxima, CL_SL_Min and its frequency, CL_SL_Nu; as well as the frequency of SL_Max, SL_Nu. The figure was made by analyzing the modified sinc, from equation 7, across the following values: w_P, 200, 240 and 280nm; w_A, 60, 90 120nm; T_A, 0.6, 0.8 and 1.0; Δx, 280, 420 and 560nm; and a wavelength of 248nm. As shown in Figure 4, shaping the sinc function of the primary feature shows the following dependencies: w_P affects
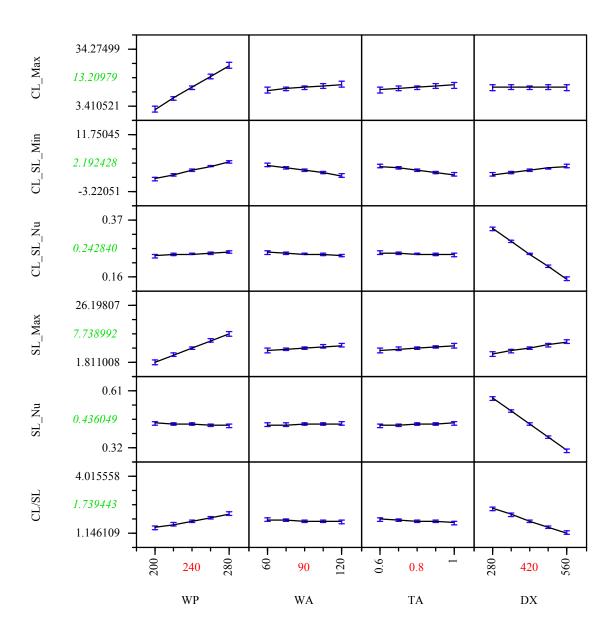
Figure 4 This figure shows how the sinc function is modified by the different parameters in Equation 7. The figure shows the relationship of w_P, w_A, T_A and Δx to the maximum amplitudes of the central and side-lobes, CL_Max and SL_Max, respectively, their ratio CL/SL; the minimum amplitude between the central-lobe and side-lobe maxima, CL_SL_Min and its frequency, CL_SL_Nu; as well as the frequency of SL_Max, SL_Nu. The figure was made by analyzing the modified sinc, from equation 7, across the following values: w_P, 200, 240 and 280nm; w_A, 60, 90 120nm; T_A,0.6, 0.8 and 1.0; Δx,280, 420 and 560nm; and a wavelength of 248nm.
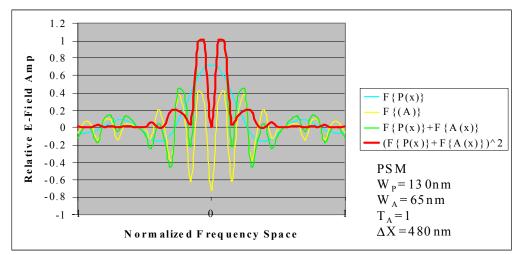
primarily the magnitude of the central-lobe and, secondly, the magnitude of the side-lobes.

Thirdly, the magnitude of the side-lobe is directly related to Δx. The frequency of the side-lobe maximum is inversely related to Δx thus showing a relationship to pitch. This relationship, in turn, holds true for the minimum amplitude between the two maxima, as

well as their ratio. To a lesser degree, relative to w_P and Δx, w_A and T_A directly affect the magnitudes of the lobes; however, they do inversely affect the minimum between the lobes. It is this latter affect that makes it important to make w_A as large as possible without allowing it to form a resolvable image by reducing T_A and/or by limiting the size to about half of w_P. Also, as will be shown later, adding additional pairs of assist features spaced at an integer multiple of Δx will further help reduce the minimum between the lobes. Empirically, Chen showed that k_1 should be around 0.20 to 0.25 for w_A, which equals $w_A \cdot NA/\lambda$. and 0.55 to 0.75 for primary-to-assist feature separation, which equals $(\Delta x - 0.5 \cdot (w_P + w_A)) \cdot NA/\lambda$.[20]

The attributes of the modified sinc function are the following: First, with proper tuning of all the lobes the feature can be made to print the same size as the dense feature, hence its use as an OPC structure. Second, image printability improves because the trimming of the primary sinc reduces the set of non-optimal angles that interfere to form the image at the image plane of the wafer. In the bright field, this improvement gives rise to an increase in depth of focus, and the reduction of MEEF.[17, 18, 19, 20] For the same reason, modifying the sinc reduces sensitivity to aberrations by decreasing the affects of aberrated beams with non-optimal interference angles.[20]

Finally, the modified sinc improves the performance of off-axis illumination, not only by reducing non-optimal interference but also by maximizing the interference that does occur by setting the frequency to match the frequency of the dense line diffraction pattern for which the illuminator was designed. These attributes make scattering and anti-scattering bars important image process integration tools for extending production resolution.

Phase-Shift Examples

For phase-shift masks, the dark field solution is shown by its components in

Figure 5 Plot of relative electric field amplitude and the square of the amplitude versus relative frequency, for n=10 for 130nm isolated space with 65nm assist features and complex transmittance of one. The amplitude is relative to the maximum amplitude of $F\{m(x)\}^2$. The curves show relative E-field amplitude contributions from the sinc function $F\{P(x)\}$, which is the transform of the primary feature, and from the sinc-shaped cosine function $F\{A(x)\}$ which is the transform of the assist features. Also shown are the sum of all the transforms, $F\{P(x)\} + F\{A(x)\}$, and the square of that sum, $F\{m(x)\}^2 = (F\{P(x)\} + F\{A(x)\})^2$.

Figure 5. This is a plot of relative electric field amplitude and the square of the amplitude versus relative frequency, for n=10 for a 130nm isolated space with 65nm assists and complex transmittance of one. The amplitude is relative to the square of the maximum amplitude of $F\{m(x)\}^2$. Figure 5 has four curves, the transform of the primary feature, the transform of the combined assist features, which is a cosine shaped by the assist feature sinc, the sum of the all Fourier transforms and the square of that sum. The sum of all the transforms is a function that has side-lobes symmetrical placed around zero frequency with amplitude that is generally less than its binary mask analog. As shown in Figure 5, in this design the electric field of the assist features can be manipulated to be equal but opposite of the primary, thus zeroing the amplitude of the central lobe. Under these conditions, the modified sinc function matches the frequency and amplitude of a strong phase-shifted feature.

At first glance this diffraction patterns looks like the discrete diffraction pattern of a infinite series of lines and spaces whose zero order has been removed by an opaque aperture in the pupil plane of the lens. This type of imaging is known as dark field. If this was really dark field imaging only the edges of the feature would be resolved and we would not know if this image was a series of small spaces and large lines or the other way around. However, this is not the discrete diffraction pattern of a series of lines and spaces but a modified sinc diffraction pattern of an isolated line described by equation 9. For that reason, it still contains information of an isolated space and produces the corresponding photoresist image.

A strong phase-shifted type image forms by interfering the two lobes of the modified sinc function when they are brought back together at the image plane. Because the lobes are symmetric about the center of the optical axis the beams maintain a uniform interference relationship when equally aberrated, as in the case where the imaging material is moved in or out of the best image plane. This invariance in the interference relationship with focus gives rise to better stability of the size and shape of the final resist image. In fact, with respect to spatial coherence, if the lobes were points with no radial distribution about their nodal centers, the depth of focus would be infinite. However, since the nodes are not points and energy distribution exists away from the nodal center, the interference from these off center components reduce the focus tolerance to something less than infinite, but one that is still significantly better than the depth of focus of a unmodified sinc function or of a modified function whose phase-shifted electric fields are not perfectly balanced. The nodal center frequency is also important. This is because of complex phase relationships about the center of each node that are best trimmed using the numerical aperture of the lens as a low pass frequency filter to get best performance. Figure 6 show simulated exposure latitudes and depth of focus comparison of a 240nm isolated space imaged with and without 120nm assist features, a Δx of 300nm and T_A of 1.0 for the strong shift and 0.5 for the weak shift. The figure also includes the diffraction pattern convolved with the source. The simulations were made with PROLITH's lumped parameter model (FINLE Technology), the parameters were 0.5 NA, 365nm wavelength, 0.3 sigma, contrast of 23, film thickness of 700nm, absorbance of 0.2 per micron and diffusion length of 10nm. With no assists, the depth of focus is 0.15 and 0.85 μm with limits of 10% and 5% respectively. The weak shifted mask had focus latitudes of 0.88 and 1.15 μm and the strong, 1.18 and 1.38 μm for the same respective limits to exposure latitude. The primary issue whether the strong phase-shift case is used
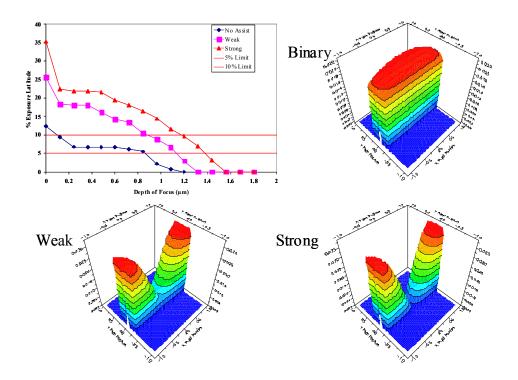
Figure 6 shows simulated exposure latitudes and depth of focus comparison of a 240nm isolated space imaged with and without 120nm assist features, a *Δx* of 300nm and *T_A* of 1.0 for the strong shift and 0.5 for the weak. The figure also includes the diffraction pattern convolved with the source. The simulations were made with PROLITH's lumped parameter model, with parameters 0.5 NA, 365nm wavelength, 0.3 sigma, contrast of 23, film thickness of 700nm, absorbance of 0.2 per micron and diffusion length of 10nm.

depends on the ability of the resist not to partially print the assist features and/or the ability to keep the CL/SL large by proper manipulation of Equation 8 or 9.

The frequency where the center of each node is located is driven by the distance *Δx*. The smaller this value, the greater the absolute frequency value. Figure 7 shows how the focus tolerance changes with nodal position in frequency space. In this figure, the vertical axis shows the percent exposure range about the dose to size a 130nm clear isolated feature with respect to frequency for varying amounts of defocus. Typically, for an exposure tool with 0.70 numerical aperture and 248nm exposure wavelength and partial coherence of 0.3, a process is said to be production worthy if the exposure latitude is greater than or equal to 5% and has a focus tolerance of more than 0.4 microns. In figure 7, this occurs when the normalized frequency is larger than 0.6, with optimum performance at frequencies between 0.8 and 1.2. Below the frequency of 0.6, from 0 to 0.3 the performance is the same as an unmodified sinc function and the phase shifter provides no enhancement. Between frequencies of 0.3 and 0.6, the performance is worse than if no phase shifting was used. This degradation appears to be related to the introduction of 180-degree phase component of the node and the width of this phase region defined by the partial coherence of the imaging system. This phase component is
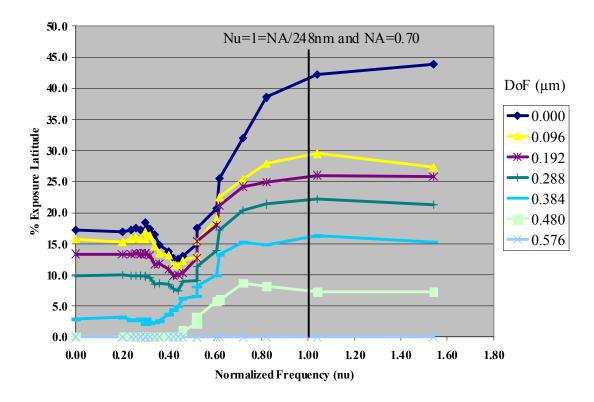
Figure 7 Percent exposure latitude for different amounts of defocus form 0.000 to 0.576 microns.

not observed at frequencies greater than 0.92 for coherent light, but with partially coherent illumination it would be first introduced at 0.92 minus 0.3, the coherence in this example for a value of 0.62. This means that not only does zero frequency need to be reduced to zero for the best imaging to occur but that the phase-shifted assist feature must be placed properly to remove any unwanted phase component.

To make a strong shifter, the sum of the complex transmittance and the width for the assist features is designed to cancel the electric field of the primary feature so that the amplitude at zero frequency is zero. Equation 11 shows that for the simple case of one pair of assist features that this occurs when:

Equation 11 $$T_P \cdot w_P = 2 \cdot T_A \cdot w_A$$

Further the assist features are placed close enough to the primary feature to place the side-lobes of the Fourier transform at frequencies greater than 0.6 and less than or equal to a frequency defined in Equation 12:

Equation 12 $$v \leq \frac{(1 + \alpha \cdot \sigma) \cdot \Delta x \cdot NA}{\lambda}$$

Where σ and NA equal, respectively, the partial coherence and numerical aperture of the exposure tool. And, α is a factor bigger than one that takes into account that the side-lobe has a width that is defined by the variables in equations 8 and 9.

Multiple pairs of assist features

Multiple pairs of assist features can be used. For the binary case adding assist features at multiples of Δx equal to the pitch of the most critical pitch, will sharpen the side-lobes, but will change the relative amplitudes of the lobes. Analytically, this is done simply by adding the additional assist feature transforms at their respective Δx. An example of a binary pattern is shown in Figure 8. For phase-shifting, multiple assist features can be used, as long as the sum of the Fourier transform of all features still adds to zero amplitude at zero frequency within manufacturing tolerances. This occurs when the phase of the assist feature near the primary equals the phase of the outer feature. An example is shown in Figure 9.
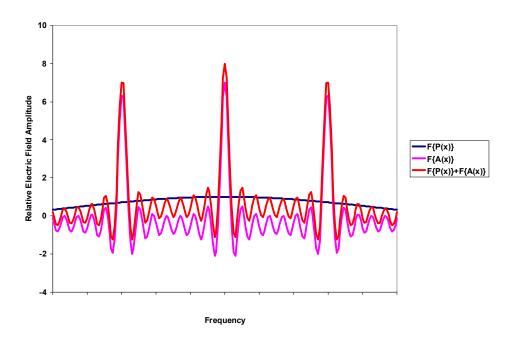

Figure 8 Fourier transforms of a binary mask with 130nm primary and seven pairs of 65nm assist features with Dx of 297.5nm. F{P(x)} is the transform of the primary. F{A(x)} is the transform of the seven pairs of assist features. F{P(x)} + F{A(x)} is the sum of all transforms. The amplitude is relative to F{P(x)}. Frequency is ±2NA.

Conclusions

Analytical solutions for the use of single set and multiple sets of sub-resolution assist features were shown. Then examples were provided for both binary and phase shift cases. It is shown that the resulting diffraction pattern is a modified sinc function and not a discrete order characteristic of a infinite Fourier series of lines and spaces. This key attribute makes it possible to do diffraction matching optical proximity compensation.

Furthermore, these attributes suggest that MEEF reduction and improved off-axis illumination is due to trimming non-optimal frequencies from the sinc function of the
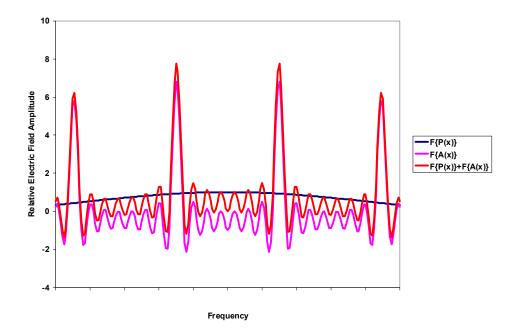

Figure 9 Fourier transforms of a phase-shift mask with 130nm primary and seven pairs of 65nm assist features with Δx of 297.5nm. In this mask the first pair of assists, nearest the primary, are shifted 180 degrees then each subsequent pair's phase is alternated. F{P(x)} is the transform of the primary. F{A(x)} is the transform of the seven pairs of assist features. F{P(x)} + F{A(x)} is the sum of all transforms. The amplitude is relative to F{P(x)}. Frequency is ±2NA.

primary feature. In closing this work suggests that frequency space needs to be considered more rigorously during pattern layout and when integrating the mask layout with the rest of the imaging process.

Acknowledgements

I would especially like to thank Chris Mack of FINLE Technologies for our extensive discussions about the nature of the modified sinc function and for the use of PROLITH. I would also like to thank J. Fung Chen and Bob Socha of ASML MaskTools and Bruce Smith of Rochester Institute of Technology for many useful discussions.

References

[1] B. E. A. Saleh and S. I. Sayegh, T. Opt. Soc. Am. 70(12), p. 1580 (1980).
[2] M. D. Prouty, Proc. SPIE Vol. 470, p. 228-232 (1984).
[3] T. Terasawa, et al, Proc. SPIE Vol. 1088, p. 25-33 (1989).
[4] I. Hanyu, et al, Proc. SPIE Vol. 1264, p. 167-177 (1990).
[5] J. G. Garofalo, et al. Proc. SPIE Vol. 1463, p. 151-166 (1991).
[6] M. Op de Beeck, et al, Proc. SPIE Vol. 1463, p. 180-196 (1991).
[7] Y. Liu, Proc. SPIE Vol. 1927, p. 477-493 (1993).

[8] S. Matsuura, et al, Proc. SPIE Vol. 3051, p. 245-256 (1997).

[9] J. S. Petersen, et al, Proc. SPIE Vol. 3546, p. 288-303 (1998) and J. S. Petersen, et al, Proc. SPIE Vol. 3741, p. 73-89 (1999).

[10] N. Kachwala, J. S. Petersen, et al, Proc. SPIE Vol. 3679, p. 55-67 (1999).

[11] R. J. Socha, et al, Proc. SPIE Vol. 3748, p. 290-314 (1999).

[12] J. F. Chen, et al, Proc. SPIE Vol. 3051, p.790 - 803 (1997).

[13] J. F. Chen, et al, Proc. SPIE Vol. 3236, p. 382-396 (1997).

[14] J. F. Chen, et al, Proc. VDE, p.177 - 192 (1997).

[15] J. F. Chen, et al, JVST B 15(6), Nov/Dec p. 2426 - 2433 (1997).

[16] J. S. Petersen, et al, Proc. SPIE Vol. 3412, p. 503-520 (1998).

[17] K. Adam, et al, Proc. SPIE Vol. 3546, p. 642-650 (1998).

[18] J. Randall, A. Tritchkov, EIPBN 98, JVST B Nov/Dec, p. 3606-3611 (1998).

[19] R. Jonckheere, et al, SPIE Vol. 3546, p. 313-324 (1998).

[20] J. F. Chen, et al, Proc. SPIE Vol. 3873, p. 995-1016 (1999).

[21] G. Vandenberghe, et al, SPIE. Vol. 3679, p. 228-238 (1999).

[22] Raymond G. Wilson, _Fourier Series and Optical Transform Techniques in Contemporary Optics_, John Wiley & Sons, Inc., New York, NY, ISBN 0-471-30357-7, p. 229-234 (1995).